

Multi-Scale Analyses of Landscape: New Tools for Studying the Effect of Erosion and Deposition on Landscape Morphology and Complexity

Christopher Keylock¹, Arvind Singh², Paola Passalacqua³, and Efi Foufoula-Georgiou⁴

¹University of Loughborough

²University of Central Florida

³University of Texas at Austin

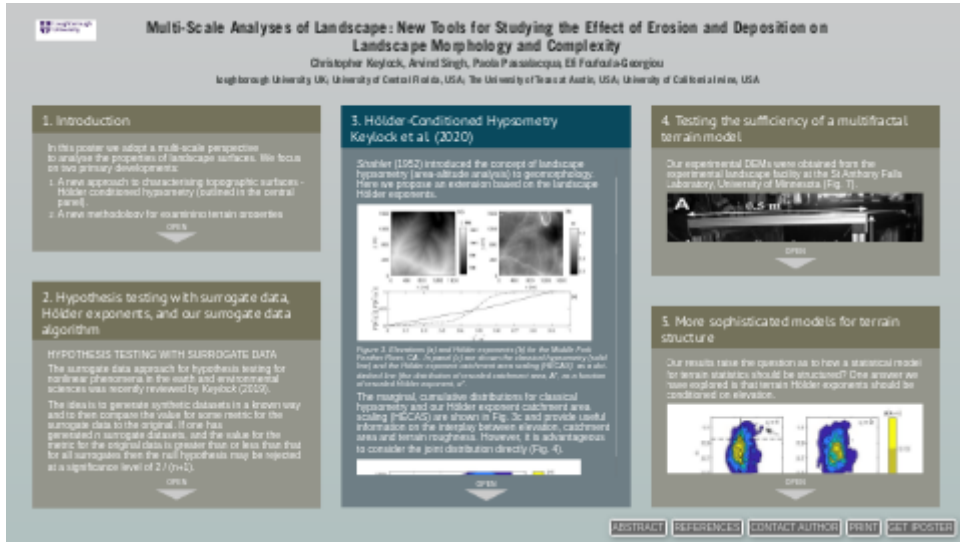
⁴University of California Irvine

November 23, 2022

Abstract

Understanding the complex interplay between erosional and depositional processes, and their relative roles in shaping landscape morphology is a question at the heart of geomorphology. A unified framework for examining this question can be developed by simultaneously considering terrain elevation statistics over multiple scales. We show how a long-standing tool for landscape analysis, the elevation-area or hypsometry, can be complemented by an analysis of the elevation scalings to produce a more sensitive tool for studying the interplay between processes, and their impact on morphology. We then use this method, as well as well-known geomorphic techniques (slope-area scaling relations, the number of basins and basin size as a function of channel order) to demonstrate how the complexity of an experimental landscape evolves through time. Our primary result is that the complexity increases once a flux equilibrium is established as a consequence of the role of diffusive processes acting at intermediate elevations. We gauge landscape complexity by comparing results between the experimental landscape surfaces and those produced from a new algorithm that fixes in place the elevation scaling statistics, but randomizes the elevations with respect to these scalings. We constrain the degree of randomization systematically and use the amount of constraint as a measure of complexity. The starting point for the method is illustrated in the figure, which shows the original landscape (top-left) and three synthetic variants generated with no constraints to the randomization. The value quoted in these panels is the root-mean-squared difference in the elevation values for the synthetic cases relative to the original terrain. This value is greatest where the original ridge becomes a valley. All these landscapes contain the same elevation values (i.e. the same probability distribution functions), and the same elevation scalings at a point. The differences emerge because the elevations themselves are distributed randomly across the surface.

Multi-Scale Analyses of Landscape: New Tools for Studying the Effect of Erosion and Deposition on Landscape Morphology and Complexity



Christopher Keylock, Arvind Singh, Paola Passalacqua, Efi Foufoula-Georgiou

Loughborough University, UK; University of Central Florida, USA; The University of Texas at Austin, USA; University of California Irvine, USA

PRESENTED AT:



1. INTRODUCTION

In this poster we adopt a multi-scale perspective to analyse the properties of landscape surfaces. We focus on two primary developments:

1. A new approach to characterising topographic surfaces - Hölder conditioned hypsometry (outlined in the central panel).
2. A new methodology for examining terrain properties using any metric, where hypotheses concern the extent to which the terrain is a realisation of a hierarchical, multifractal phenomenon. This forms the focus of the poster, and we use Hölder conditioned hypsometry in this context.

2. HYPOTHESIS TESTING WITH SURROGATE DATA, HÖLDER EXPONENTS, AND OUR SURROGATE DATA ALGORITHM

HYPOTHESIS TESTING WITH SURROGATE DATA

The surrogate data approach for hypothesis testing for nonlinear phenomena in the earth and environmental sciences was recently reviewed by *Keylock* (2019).

The idea is to generate synthetic datasets in a known way and to then compare the value for some metric for the surrogate data to the original. If one has generated n surrogate datasets, and the value for the metric for the original data is greater than or less than that for all surrogates then the null hypothesis may be rejected at a significance level of $2 / (n+1)$.

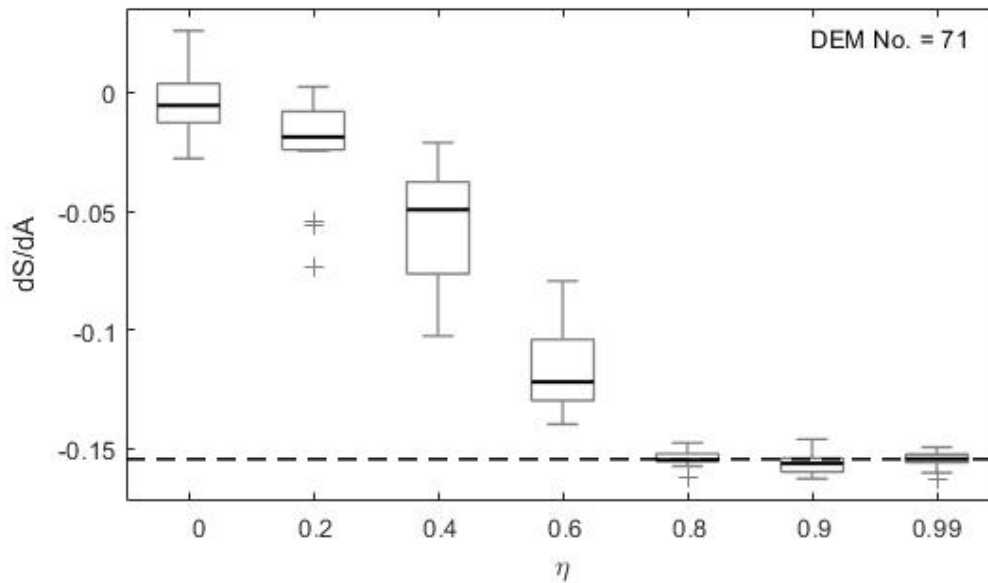


Figure 1. Gradual multifractal reconstruction of the slope area scaling relation, dS/dA , for catchments extracted from an experimental DEM. This result is discussed further in panel. 4.

Gradual reconstruction (*Keylock*, 2010; *Keylock*, 2018) generalises this idea such that synthetic data are generated on a continuum, $0 \leq \eta \leq 1$, where as $\eta \rightarrow 1$, the surrogate data converge on the original system. Hence, it is possible to determine how complex a dataset is on a given metric. Thus, in Fig. 1, a significant difference for the catchment slope-area scaling persists until $\eta \geq 0.8$.

HÖLDER EXPONENTS

A landscape where the Hölder exponent is the same everywhere would be considered as a monofractal landscape. As the scaling for the variation in topography changes from place to place, the terrain roughness changes and the Hölder exponent characterises this. Where the Hölder exponent is a function of the first derivative of elevation it is bounded $0 < \alpha < 1$, and is defined for elevations, z , in orthogonal directions, x and y as:

$$|z(x, y) - z(x + \delta, y + \delta)| \sim C|\delta|^{\alpha(x,y)}$$

where the dependence of α on spatial position is dropped from the notation in what follows.

OUR SURROGATE DATA ALGORITHM

Our iterated, amplitude adjusted wavelet transform (IAAWT) surrogate data algorithm (Keylock, 2017) retains all the original values in a dataset and its multifractal structure. Hence, it is possible to test if a multifractal description of a phenomenon is sufficient. Three realisations of a DEM using our algorithm are shown in Fig. 2. The method was generalised into a gradual reconstruction framework by Keylock (2018) by selectively fixing in place the wavelet phases of the complex wavelet transform that underpins the method.

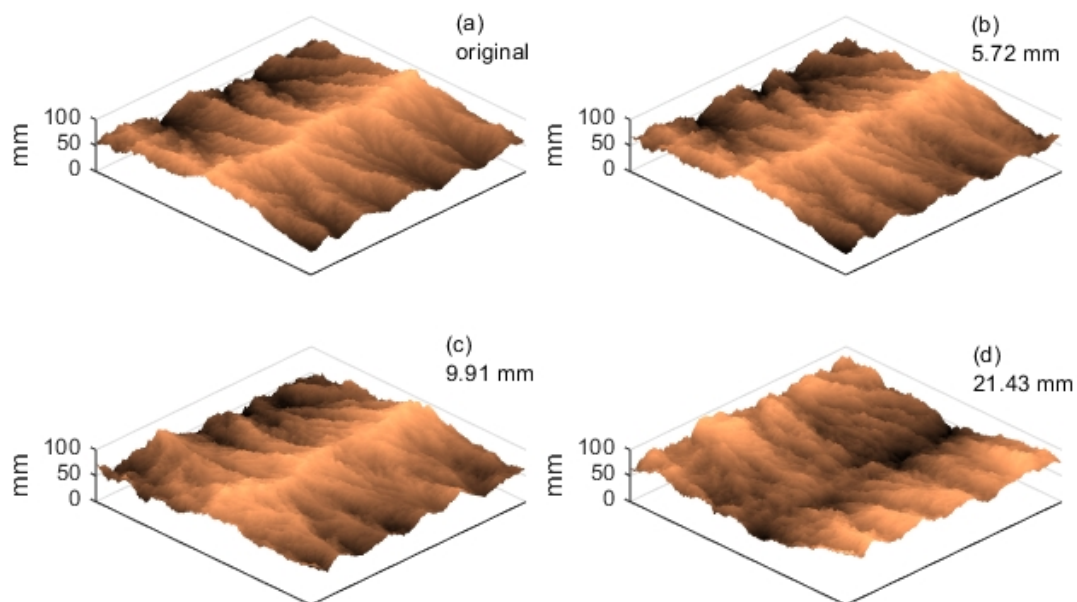


Figure 2. The original DEM (a) and three IAAWT surrogates. The value stated next to each panel is the RMSE between the original and the surrogate case, showing that the elevations are randomised even though the multifractal structure is preserved.

3. HÖLDER-CONDITIONED HYPSONOMETRY KEYLOCK ET AL. (2020)

Strahler (1952) introduced the concept of landscape hypsometry (area-altitude analysis) to geomorphology. Here we propose an extension based on the landscape Hölder exponents.

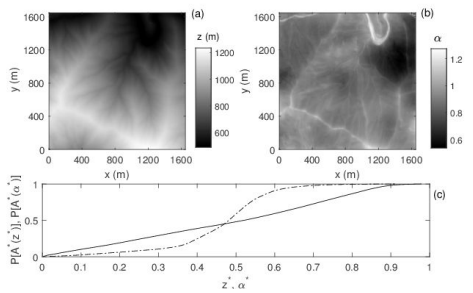


Figure 3. Elevations (a) and Hölder exponents (b) for the Middle Fork Feather River, CA . In panel (c) are shown the classical hypsometry (solid line) and the Hölder exponent catchment area scaling (HECAS) as a dot-dashed line (the distribution of rescaled catchment area, A^* , as a function of rescaled Hölder exponent, α^*).

The marginal, cumulative distributions for classical hypsometry and our Hölder exponent catchment area scaling (HECAS) are shown in Fig. 3c and provide useful information on the interplay between elevation, catchment area and terrain roughness. However, it is advantageous to consider the joint distribution directly (Fig. 4).

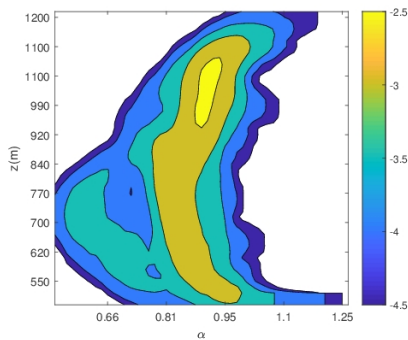


Figure 4. The joint distribution function for the elevations and Hölder exponents for the Feather River data shown using a contour plot and logarithmically-spaced contour intervals.

Based on Strahler's notion of the hypsometric integral (the integral of the solid line in Fig. 3c), we defined conditional integrals for both:

1. The elevation at a given α ($I_{hyp} | \alpha$) ; and,
2. The Hölder exponents at a given z ($I_{\alpha} | z$).

These integrals were then plotted as a function of the conditioning variable (see Fig. 5).

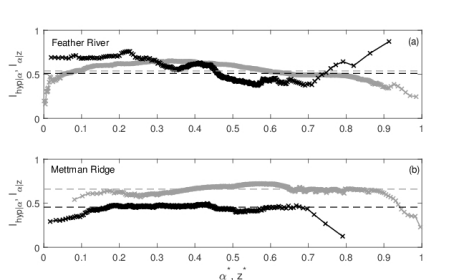


Figure 5. The two types of conditional integrals for the Feather River (a) and Mettman Ridge (b) catchments. $I_{hyp} | \alpha$ is shown in black and $I_{\alpha} | z$ is in gray. The dashed lines are the mean values. Hence, the black dashed line is Strahler's hypsometric integral.

From Fig. 5 one can study the mean values for these conditional integrals, or the moments or trends of the residuals about the mean. Using five catchments studied recently by Sangireddy *et al.* (2017), a principal components analysis gave three metrics to summarise catchment response:

- Strahler's original hypsometric integral, I_{hyp} ;
- The standard deviation of the $I_{hyp} | \alpha$ values (the variability seen in Fig. 5) denoted as $\sigma(r_{hyp})$;
- The linear trend in the $I_{hyp} | \alpha$ values as a function of α^* (the slope for the results in Fig. 5) denoted as $\theta(r_{hyp})$.

It is clear in Fig. 6 that the different catchments, all of which have a mature topography according to Strahler's original classification, can be readily distinguished using these three terms. Of the five drainage basins, only Mettman Ridge (see Fig. 5) is truly described by Strahler's hypsometric integral, i.e. $\sigma(r_{hyp}) \rightarrow 0$ and $\theta(r_{hyp}) \rightarrow 0$.

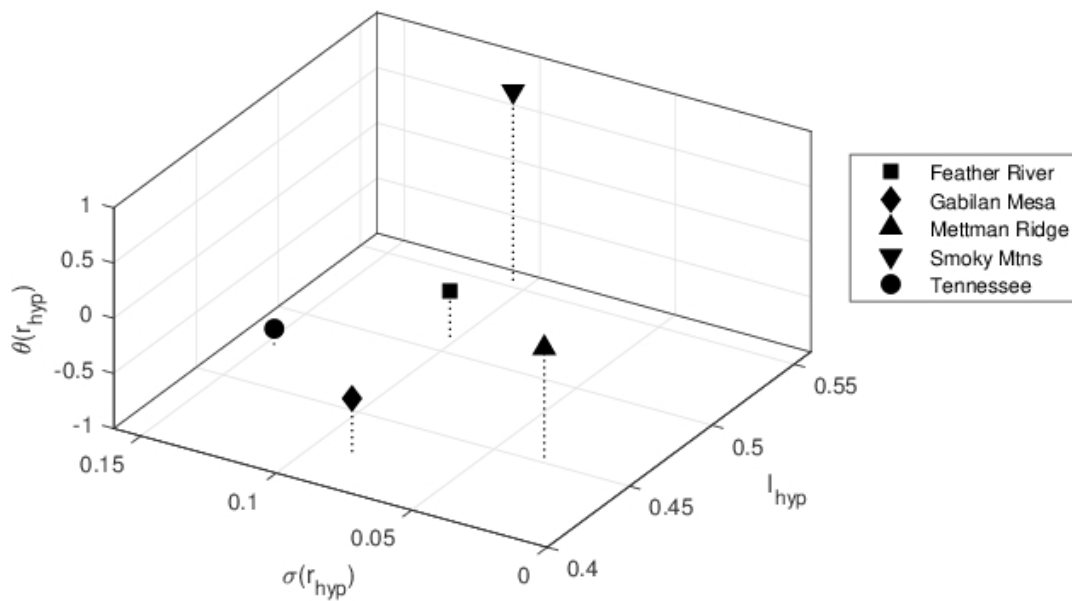


Figure 6. The locations of the five catchments studied by Sangireddy *et al.* (2017) in a three-dimensional space formed from our selected measures of hypsometry: I_{hyp} , $\sigma(r_{hyp})$, and $\theta(r_{hyp})$.

4. TESTING THE SUFFICIENCY OF A MULTIFRACTAL TERRAIN MODEL

Our experimental DEMs were obtained from the experimental landscape facility at the St Anthony Falls Laboratory, University of Minnesota (Fig. 7).

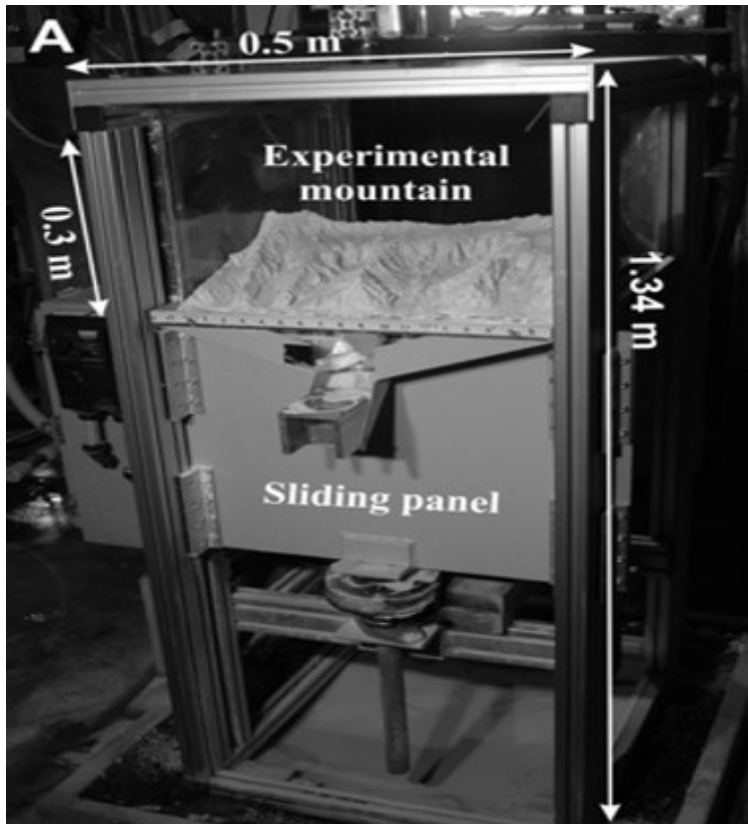


Figure 7. The experimental facility in Minnesota. Rain droplets are smaller than $10\ \mu\text{m}$. A laser scanner resolved the topography at $0.5\ \text{mm}$ resolution every $300\ \text{s}$.

The evolution of the topography can be seen in Fig. 8, where each unit of time equates to the $300\ \text{s}$ sampling interval.

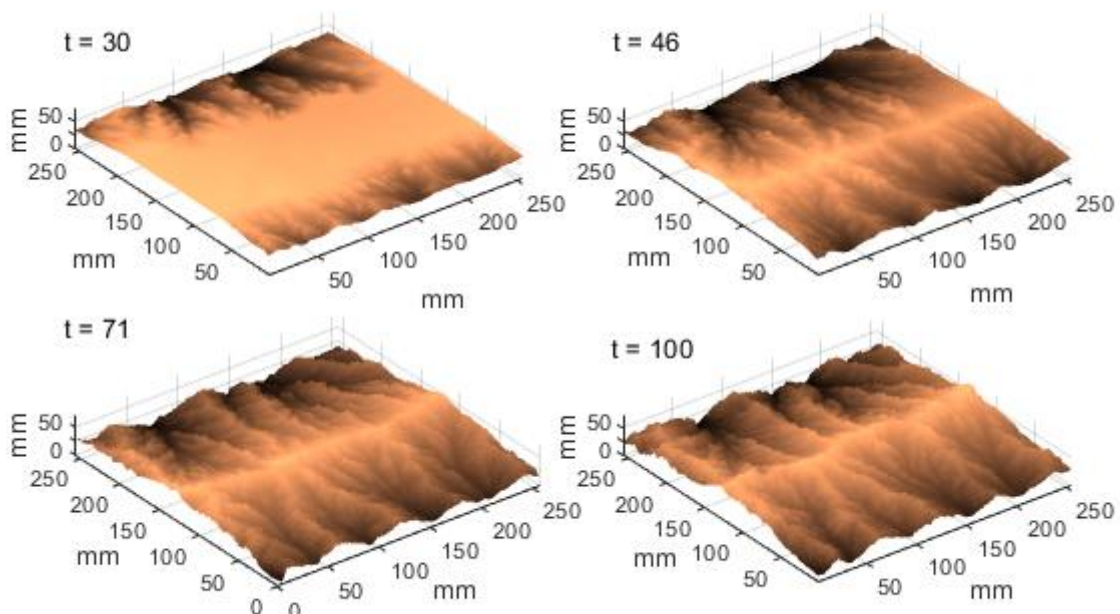


Figure 8. The evolution of the experimental topography over time. The image at $t = 100$ is identical to that in the top-left in Fig. 2.

For 22 DEMs we determined the values for a number of well-known terrain metrics such as the scaling relation between catchment slope and catchment area, dS/dA , as well as the number and total channel length, ΣL of basins of a given Horton-Strahler order, Ω . The overall conclusion from these analyses was that the multifractal model for terrain, i.e. $\eta = 0$, is unable to replicate the observed characteristics. For example, Fig. 9 shows the slope-area scaling relations for the four DEMs shown in Fig. 8. It is clear that $\eta \gg 0$ in order for there to be no significant difference between data and surrogates.

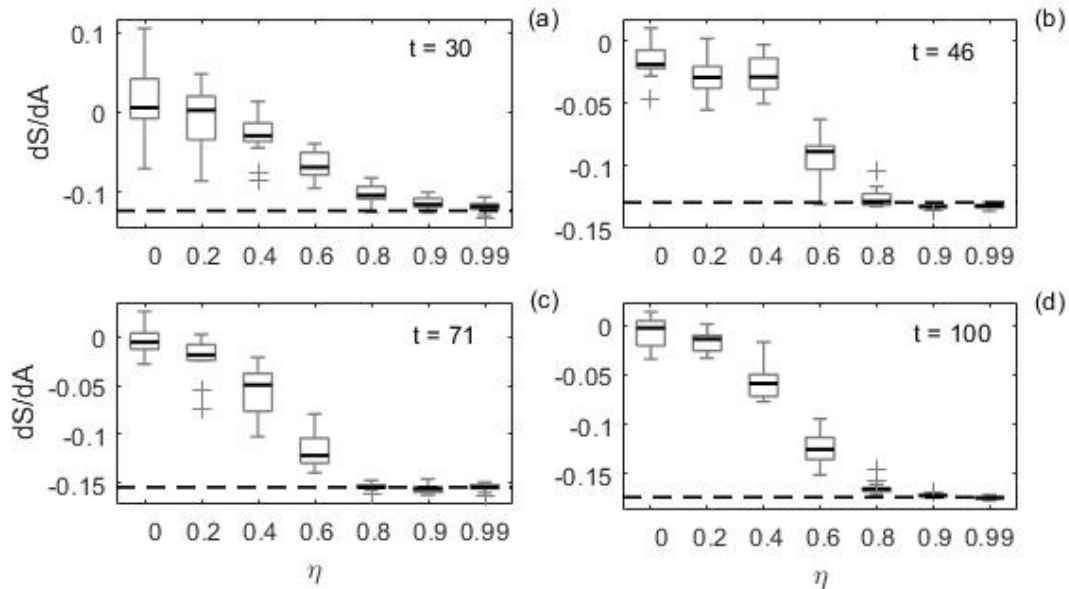


Figure 9. Gradual multifractal reconstruction of the slope-area scaling relation, dS/dA as a function of η and time. The panels correspond to those in Fig. 8. The dashed horizontal line is that for the original data from Fig. 8. The boxplots indicate the values for the surrogate data.

There was also some evidence that this threshold value continued to increase, even when the landscape had achieved a flux equilibrium (from about $t = 70$), as shown in Fig. 10. Thus, these landscapes are statistically significantly more complex than a multifractal model would imply.

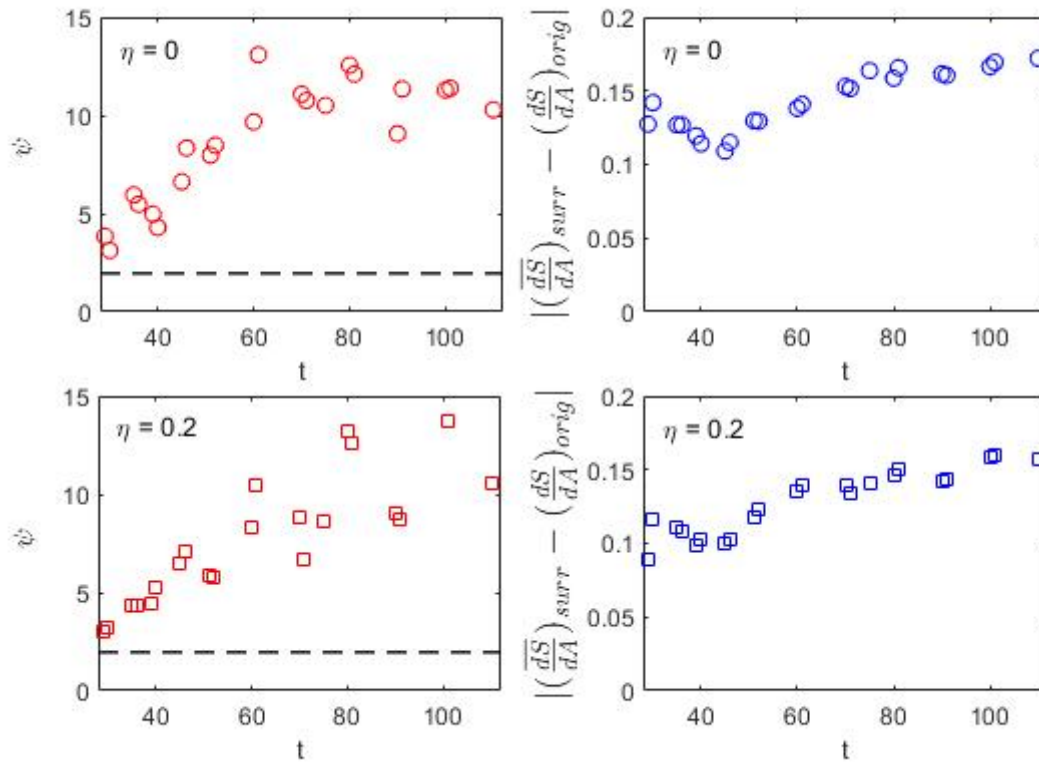


Figure 10. The absolute distance between the mean value for the surrogate data and the original data for two choices of η . The panels on the right-hand side show the unnormalized distances, while the panels on the left make use of the quantity, ψ , which is the quantity in the right-hand panels divided by the standard deviation of the values for the surrogates. The dashed line represents a 5% significance level for a normally distributed variate.

5. MORE SOPHISTICATED MODELS FOR TERRAIN STRUCTURE

Our results raise the question as to how a statistical model for terrain statistics should be structured? One answer we have explored is that terrain Hölder exponents should be conditioned on elevation.

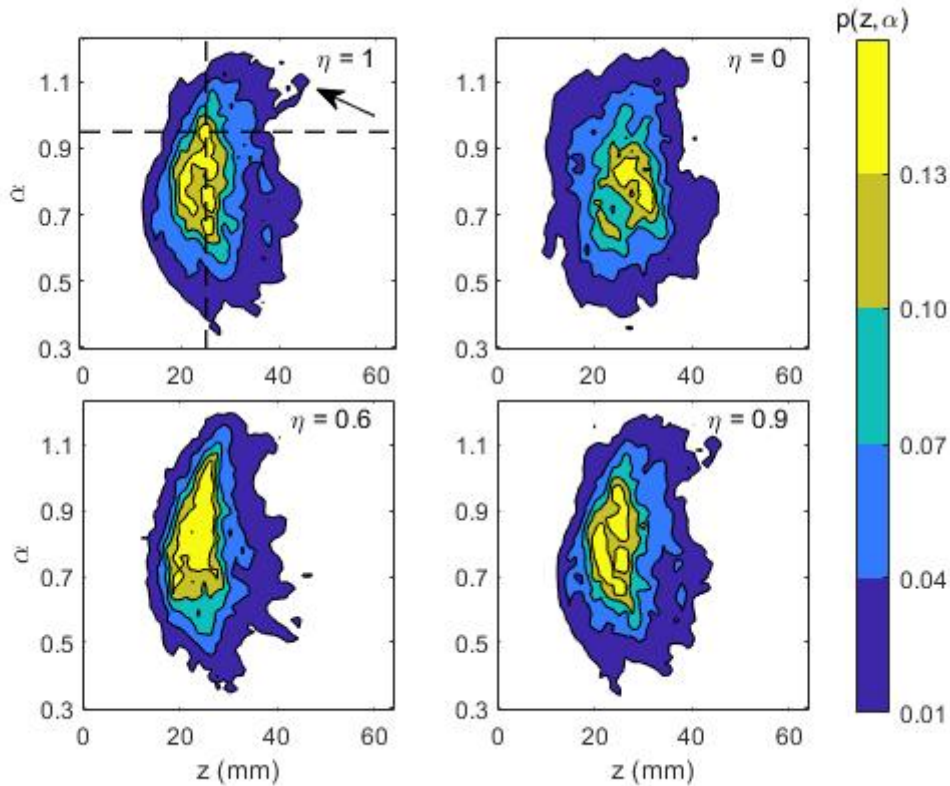


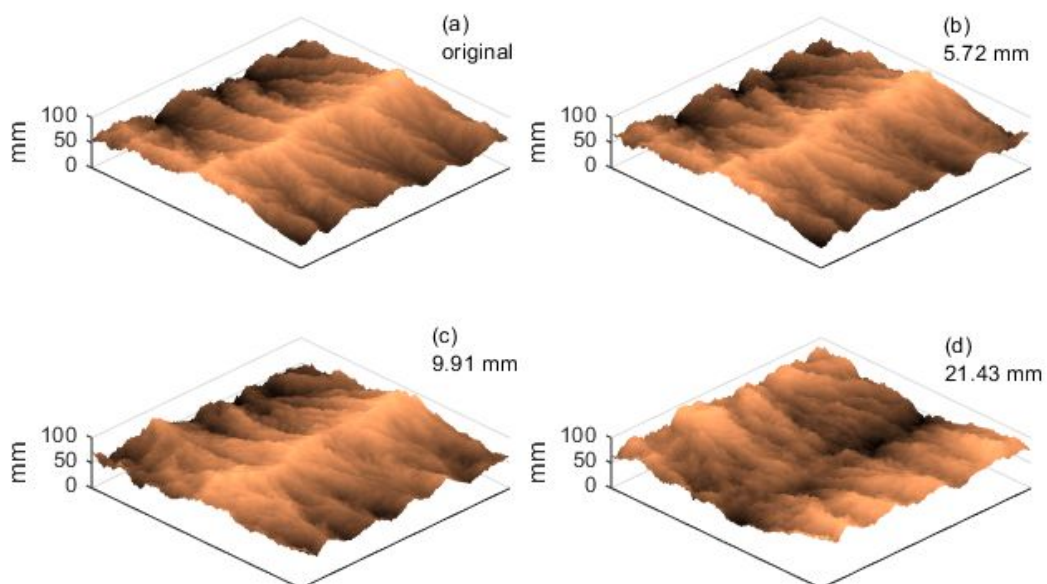
Figure 11. Joint distribution functions for elevation and Hölder exponents similar to Fig. 4 but for the experimental DEM at $t = 100$. The top-left panel shows the results for the original data ($\eta = 1$), while the other panels show the distribution at other values for η .

Using our gradual reconstruction framework, it is clear from Fig. 11 that for the DEM extracted at $t = 100$, one needs $\eta \sim 0.9$ in order to capture the key features of the joint distribution for elevation and Hölder exponents, including the feature highlighted by the arrow in the top-left panel. Thus, while the landscape is clearly not a simple multifractal, the recent theory of self-regulating stochastic processes (Levy-Vehel, 2013) has some useful potential applications in geomorphology for producing terrain models with appropriately conditioned Hölder exponents.

ABSTRACT

Understanding the complex interplay between erosional and depositional processes, and their relative roles in shaping landscape morphology is a question at the heart of geomorphology. A unified framework for examining this question can be developed by simultaneously considering terrain elevation statistics over multiple scales. We show how a long-standing tool for landscape analysis, the elevation-area or hypsometry, can be complemented by an analysis of the elevation scalings to produce a more sensitive tool for studying the interplay between processes, and their impact on morphology. We then use this method, as well as well-known geomorphic techniques (slope-area scaling relations, the number of basins and basin size as a function of channel order) to demonstrate how the complexity of an experimental landscape evolves through time. Our primary result is that the complexity increases once a flux equilibrium is established as a consequence of the role of diffusive processes acting at intermediate elevations.

We gauge landscape complexity by comparing results between the experimental landscape surfaces and those produced from a new algorithm that fixes in place the elevation scaling statistics, but randomizes the elevations with respect to these scalings. We constrain the degree of randomization systematically and use the amount of constraint as a measure of complexity. The starting point for the method is illustrated in the figure, which shows the original landscape (top-left) and three synthetic variants generated with no constraints to the randomization. The value quoted in these panels is the root-mean-squared difference in the elevation values for the synthetic cases relative to the original terrain. This value is greatest where the original ridge becomes a valley. All these landscapes contain the same elevation values (i.e. the same probability distribution functions), and the same elevation scalings at a point. The differences emerge because the elevations themselves are distributed randomly across the surface.



(https://agu.confex.com/data/abstract/agu/fm20/5/0/Paper_663705_abstract_637923_0.jpg)

REFERENCES

- Keylock, C. J.** (2010). Characterizing the structure of nonlinear systems using gradual wavelet reconstruction. *Nonlinear Processes in Geophysics*, 17, 615–632.
- Keylock, C. J.** (2017). Multifractal surrogate-data generation algorithm that preserves pointwise Hölder regularity structure, with initial applications to turbulence, *Phys. Rev. E*, 95, 032123, doi:10.1103/PhysRevE.95.032123 (<https://doi.org/10.1103/PhysRevE.95.032123>)
- Keylock, C. J.** (2018). Gradual multifractal reconstruction of time-series: Formulation of the method and an application to the coupling between stock market indices and their Hölder exponents. *Physica D: Nonlinear Phenomena*, 368, 1-9. doi: 10.1016/j.physd.2017.11.011 (<https://doi.org/10.1016/j.physd.2017.11.011>)
- Keylock, C. J.** (2019). Hypothesis testing for nonlinear phenomena in the geosciences using synthetic, surrogate data. *Earth & Space Science*, 6, 41–58, doi: 10.1029/2018EA000435 (<https://doi.org/10.1029/2018EA000435>)
- Keylock, C.J., Singh, A., Passalacqua, P., Foufoula-Georgiou, E.** (2020). Hölder-Conditioned Hypsometry: A Refinement to a Classical Approach for the Characterization of Topography, *Water Resources Research*, 56, doi: 10.1029/2019WR025412 (<https://doi.org/10.1029/2019WR025412>)
- Levy-Vehel, J. (2013), Beyond multifractional Brownian motion: New stochastic models for geophysical modelling, *Nonlinear Processes in Geophysics* 20(5), 643-655.
- Sangireddy, H., Stark, C. P., & **Passalacqua, P.** (2017). Multiresolution analysis of characteristic length scales with high-resolution topographic data. *Journal of Geophysical Research: Earth Surface*, 122, 1296-1324, doi: 10.1002/2015JF003788 (<https://doi.org/10.1002/2015JF003788>)
- Singh, A., Reinhardt, L. and Foufoula-Georgiou, E.** (2015), Landscape reorganization under changing climatic forcing: Results from an experimental landscape, *Water Resources Research* 51, 4320-4337, doi:10.1002/2015WR017161 (<https://doi.org/10.1002/2015WR017161>).
- Strahler, A. N. (1952). Hypsometric (area-altitude) analysis of erosional topography. *Geological Society of America Bulletin*, 63, 1117–1142.